J Ind Microbiol Biotechnol (2015) 42:735–744
DOI 10.1007/s10295-015-1601-1

ENVIRONMENTAL MICROBIOLOGY

SIMB
Society for Industrial Microbiology and Biotechnology

Concentration- and roughness-dependent antibacterial and antifungal activities of CuO thin films and their Cu ion cytotoxicity and elution behavior

Gyu-In Shim · Seong-Hwan Kim · Hyung-Woo Eom · Se-Young Choi

Received: 22 August 2014 / Accepted: 13 February 2015 / Published online: 24 February 2015
© Society for Industrial Microbiology and Biotechnology 2015

Abstract In this study, we aimed to evaluate the antibacterial and antifungal properties, cytotoxicity, and elution behavior of copper oxide (CuO) thin films with varying concentrations and roughness values. CuO films greater than 0.2 mol % showed 99.9 % antimicrobial activity against *Escherichia coli*, *Staphylococcus aureus*, *Campylobacter jejuni*, and *Penicillium funiculosum*. Cu ions were found to be noncytotoxic in New Zealand white rabbits. The concentration of Cu ions from CuO thin films eluted in drinking water in 24 h at 100 °C was 0.014 μg L^{-1}, which was below the standard acceptable level of 0.02 μg L^{-1}. The transmittance of CuO thin film-coated glass was similar to that of parent glass. The antimicrobial activity, cytotoxicity, elution behavior, and transmittance of CuO deposited on glass suggest that these films could be useful in household devices and display devices.

Keywords Copper oxide film · Antimicrobial activity · Cytotoxicity · Elution behavior

Introduction

In the last decade, interest in environmentally friendly home electronics as well as bathroom and kitchen products has increased greatly. In addition to the goal of improving our standard of living, the requirement for household cleanliness has increased with the increasing human lifespan. Despite our interest in maintaining healthy lifestyles, germs pose a serious challenge to healthy living [7, 23]. Therefore, the antimicrobial properties of metal ions on glass, bulk metallic glass, plastic, and steel are now being actively investigated [13, 16, 29]. Common metal ions such as Zn^{2+}, Cu^{2+}, Al^{3+}, and Ag^{+} exhibit antimicrobial properties [2, 10, 13, 15, 21]. These materials are used as disinfectants against various kinds of microbes. Ag^{+} has been used most commonly as an antibacterial agent because of its many advantages, including its potent antibiotic activity and durability [3, 31]. However, a risk of dermatosis exists when the skin is exposed to Ag-coated materials [8]. Ag^{+} ions have also been reported to accumulate in the body after absorption [4, 14].

Cu ions are also an effective antimicrobial; Cu metal and Cu-based compounds are highly destructive to microbes and exhibit strong antibacterial properties [13–15]. Generally, metallic Cu has excellent antibacterial activity, more so than CuO film [6, 22]; however, CuO films have many advantages for use in display devices. For example, the processing temperature of CuO film is lower (approximately 200–400 °C) than that of metallic Cu (800–1200 °C), and oxide forms such as CuO have relatively low refractive indexes compared to that of metallic materials. Therefore, CuO films have high transmittance of light in the visible range. Moreover, CuO films with monoclinic structures have more Cu atoms on the surface than those with cubic structures; therefore, CuO film has antimicrobial activity superior to that of Cu_2O film. The raw materials used to obtain Cu ions for household applications are cheaper than those used to obtain Ag ions. The antimicrobial activities of Cu ions are proportionate to their concentration and surface roughness, because these factors increase the contact surface between Cu ions and microbes. Therefore, the use of Cu ions as an antimicrobial coating method has been investigated in several studies [11, 17–20].

G.-I. Shim · S.-H. Kim · H.-W. Eom · S.-Y. Choi (✉)
Department of Advanced Materials Science and Engineering, Yonsei University, 50 Yonsei-ro, Seodaemun-gu, Seoul 120-749, Republic of Korea
e-mail: sychoi@yonsei.ac.kr

An important advantage of the sol-coating method is the ability to precisely control film thickness and roughness by regulating spinning, dipping, and spray coating conditions such as the sol concentration, deposition speed, and heat treatment temperature [12, 26, 30]. The antimicrobial activity of Cu ions is well documented, but few studies have examined their cytotoxicity and harmful effects on the human body. High metal ion concentrations are being used in the production of various products including those that directly contact the skin; thus, the concern over Cu ion toxicity via skin absorption is growing. Prolonged Cu ion inhalation and skin contact is associated with risks such as skirt ulcer, hemochromatosis, and chronic gastritis [1]. Based on health concerns, the World Health Organization (WHO) has limited Cu requirements of human body to 2.0 mg, and restricted the maximum allowable extracting concentration of Cu ions in drinking water to 0.02–0.1 $\mu g\ L^{-1}$, according to provisional guideline values [27]. Therefore, to evaluate whether Cu ions are safe for human and animal use, the cytotoxicity and elution behavior of Cu ions must be assessed.

The purpose of the present study was to evaluate the antibacterial and antifungal properties, cytotoxicity, and elution behavior of CuO thin films against *Escherichia coli*, *Staphylococcus aureus*, *Campylobacter jejuni*, and *Penicillium funiculosum*. In addition, the transmittance of CuO thin film-coated glass prepared with various concentrations and roughness values was measured to determine whether this material could be suitable for use in display devices such as smartphones and touch panels.

Materials and methods

Preparation of CuO thin film

Cupric nitrate hemipentahydrate [$(CuNO_3)_2{\cdot}2.5H_2O$, 99 %, Sigma-Aldrich, USA], absolute ethanol, distilled water, and nitric acid (HNO_3, 70 %, Sigma-Aldrich, USA) were used to prepare the Cu solution. From 1.0, 1.5, and 2.0 g of $(CuNO_3)_2{\cdot}2.5H_2O$, respectively, 0.2, 0.3, and 0.4 mol % solutions were prepared. Mixtures containing 0.2 mol % $(CuNO_3)_2{\cdot}2.5H_2O$ and 69.8 mol % (87.8 mL) absolute ethanol were then hydrolyzed with 29.9 mol % (11.6 mL) distilled water, and 0.1 mol % (0.1 mL) nitric acid was introduced into the 100 mL solution. To put Cu-sol into a stable state, HNO_3 solution was used to adjust the pH to 1.5, and the mixture was stirred for 24 h. Square sodium aluminosilicate glass substrates (Corning Inc., USA) each 0.7 mm thick, 10 mm wide, and 10 mm long were prepared. Thin films were generated from three 0.05 mL drops of Cu solution in ethanol by using the spin-coating method at 3000 rpm for 30 s. Films were then dried at 100 °C for 10 min, and heated at 5 K min^{-1} in an Ar (99.999 %) atmosphere by using an electric tube furnace (Lindberg Blue M, USA) at 200 °C for 10 min.

Characterization of CuO thin films

The thicknesses and morphological changes of CuO thin films and microbial cells were determined using field emission scanning electron microscopy (FE-SEM, JEOL JSM-7001F, Japan) at a 15 kV accelerating voltage. Energy dispersive X-ray spectroscopy (EDS; Inca Energy 250, Oxford Instruments, UK) with a cumulative time of 150 s was used to confirm the content of Cu ions in the CuO thin films on the surface of the glass substrates. The crystalline phase of the CuO thin film was determined by X-ray diffraction (XRD, D/MAX-2500H, Rigaku, Japan) using an Ni-filtered CuK_α radiation source ($\lambda = 1.54056$ Å) in the range of $20° \leq 2\theta \leq 80°$ at a scan rate of 4° min^{-1}. The crystalline size (L) of the films was calculated using Scherrer's equation:

$$L = \frac{K\lambda}{\beta \cos\theta}$$

where K is the Scherrer constant (0.9), λ is the wavelength of XRD radiation, β is the full width at half maximum (FWHM), and θ is the diffraction angle. The interplanar spacing (d) was calculated from the XRD patterns by using Bragg's law:

$$2d \sin\theta = n\lambda$$

where θ is the diffraction angle and λ is the wavelength of X-ray used. The average surface roughness (R_a), root mean square roughness (R_q), and peak-to-valley difference (R_t) values of the CuO thin films within a scanned area of $10 \times 10\ \mu m^2$ were confirmed with atomic force microscopy (AFM, Veeco Instruments, USA) in non-contact mode. The contact angles (CAs) of the parent glass and CuO thin films were measured with a drop shape analyzer (DSA 100, Krüss GmbH, Germany) at room temperature. The droplet volume was set to a 2.0 μL scale with at least seven water drops per specimen. A UV/VIS/NIR spectrophotometer (V-570, Jasco, Japan) was used to measure the transmittance of CuO thin film deposited on glass at wavelengths ranging from 200–800 nm, and a scan speed of 400 nm min^{-1}.

Strains and culture conditions

Escherichia coli (ATCC 8739), *S. aureus* (ATCC 6538), *C. jejuni* (ATCC 49943) and *P. funiculosum* (ATCC 11797) were used. Nutrient agar medium (Difco 0001, 3.0 g beef extract, 5.0 g peptone, 15.0 g agar, and 1.0 L distilled water adjusted to pH 7.0) was used to grow *E. coli*. Trypticase soy agar medium BBL 4311768 (17.0 g pancreatic digest of casein, 3.0 g

pancreatic digest of soybean meal, 5.0 g NaCl, 2.5 g K_2HPO_4, 2.5 g glucose, 15.0 g agar, and 1.0 L distilled water) was used to culture *S. aureus*, whereas trypticase soy agar medium BBL 211043 (15.0 g pancreatic digest of casein, 15.0 g pancreatic digest of casein, 5.0 g papaic digest of soybean meal, 5.0 g NaCl, 15.0 g Agar, 50.0 mL defibrinated sheep blood, and 0.95 L distilled water adjusted to pH 7.3) was used to grow *C. jejuni*. Potato dextrose agar medium (BBL 7149, 4.0 g potato infusion, 20.0 g dextrose, 15.0 g agar, and 1.0 L distilled water) was used to grow *P. funiculosum*.

Antibacterial and antifungal activity tests

Antimicrobial tests were performed using the ISO 22196:2011(E) method. Before the beginning of the test, all specimens and tools were sterilized in an autoclave at 121 °C for 15 min. *E. coli*, *S. aureus*, *C. jejuni*, and *P. funiculosum* were diluted to concentrations between 3.0×10^5 colony forming units per milliliter (CFU mL^{-1}) and 4.0×10^5 CFU mL^{-1}. Using the dilution plating technique, the numbers of surviving bacteria as a function of the microbe dilution cultured on solid medium were counted. Bacterial suspensions were injected onto the CuO thin film in a 24-well culture plate. After 30 s, 1.0 mL of liquid medium was poured into each well, and then transferred to an agar plate (solid culture medium) for bacterial counts. The parent samples were also transferred onto agar plates for comparisons with the diluted samples. All samples were maintained under identical conditions. Substrates containing *E. coli*, *S. aureus*, and *C. jejuni* were maintained at 37 °C and aged for 24 h in an incubator, whereas *P. funiculosum* was aged at 32 °C for 24 h. Following incubation, the numbers of surviving *E. coli*, *S. aureus*, *C. jejuni*, and *P. funiculosum* cells were counted. All tests were repeated ten times, and bacterial counts were expressed as log CFU mL^{-1}. The final data are the mean values of ten tests ± standard deviation. The antibacterial activity (R) was calculated according to the following equation:

$$R = \frac{(U_t - A_t)}{U_t} \times 100\,\%$$

where U_t and A_t express the number of visible bacteria colonies on the untreated and treated test plates (cells cm^{-2}) after 24 h.

Cytotoxicity and elution tests

Cytotoxicity testing was performed by the Korea Testing and Research Institute in accordance with ISO 10993–5:2009(E) and conformed to the guide for care and use of laboratory animals. New Zealand white (NZW) rabbits were used as an experimental animal model. The rabbit skins were epilated approximately 24 h prior to partitioning the skin into test and control sites that were each 2.5×2.5 cm^2 in size, as shown in Fig. 1. The epidermis was abraded by using the end of a needle. CuO thin film was placed in contact with intact and the abraded skin of the test site. Sterilized water was spread on the control site located at the lower part of the skin. The test and control sites were then covered with sterile gauze and were affixed using tape. The numbers of dead animals and their weight variations were monitored at 24 and 72 h after CuO exposure, as shown in Fig. 1a, b, respectively. The primary irritation index (PII) was determined using the following formula:

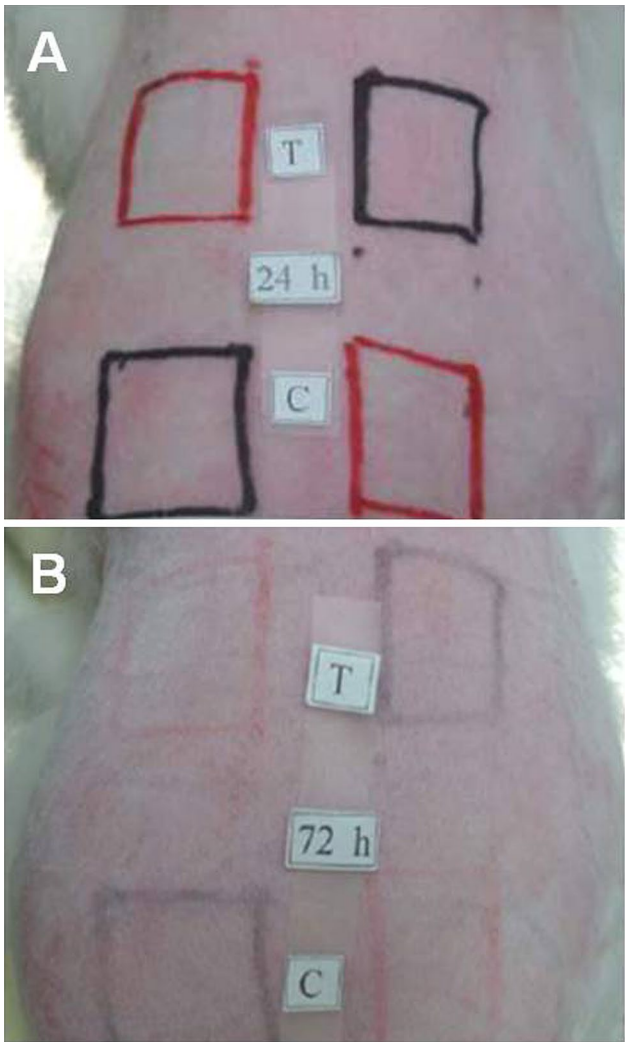

Fig. 1 Photographs of New Zealand white rabbits used for the cytotoxicity tests: **a** 24 h and **b** 72 h after incubation with 0.2 mol % Cu ions. *Red square* indicates abraded skin, *black square* showed intact skin with test (*T*) and control (*C*) sites

$$\text{PII} = \frac{\text{Sum of means of scores marked at 24 h and 72 h}}{4}$$

The PII was used to evaluate cytotoxicity and skin irritation. According to the PII value, the material was classified as being a nonirritant (PII ≤0.5), mild irritant (0.6 ≤ PII

≤ 2.0), moderate irritant (2.1 ≤ PII ≤ 5.0), or severe irritant (5.1 ≤ PII ≤ 8.0). The mean PII values were calculated from a total of 6 NZW rabbits. The elution test for the CuO film was performed using inductively coupled plasma (ICP) atomic emission spectroscopy (Optima-4300 DV, USA). To confirm that the Cu ion concentration in drinking water meets the WHO guideline (2.0 mg L^{-1}, ICP analysis limit of detection: 0.02 μg L^{-1}), the CuO (0.2–0.4 mol %) thin film-coated glass substrate was placed into drinking water (100 mL). The drinking water used for the elution test was purified water (pH 7.4 at 25 °C) containing between 0.1 and 0.5 mg L^{-1} dissolved minerals (Ca^{2+}, K^{+}, Mg^{2+}, Na^{+}). The concentration of eluted Cu ions was assessed at various time points between 1 and 24 h in the water bath at 100 °C. After the elution test at 100 °C for 24 h, changes in R_a, CA, and chemical composition of the 0.4 mol % CuO thin film were calculated to confirm the durability and residual quantity of Cu on the CuO film surface.

Results

Characterization of the CuO thin film

Figure 2 shows the XRD patterns of the films prepared using various Cu-sol concentrations heated to 200 °C. The CuO diffraction pattern was a well-ordered monoclinic structure (JCPDS no.: 80–1268). Increasing the Cu concentration of the prepared sol increased the crystalline size from 5.6 (0.2 mol % Cu) to 7.6 nm (0.4 mol % Cu), as shown in Table 1. The intensities of the crystalline phases also increased with increasing Cu concentration, due to the increase in the FWHM of the main peak. The crystalline sizes and crystallinity of the CuO thin films were strongly related to the initial copper concentration. The increase in crystalline size with increasing Cu-sol concentration can be attributed to atomic diffusion and agglomeration of the Cu in the CuO thin film during the heating process at 200 °C. In addition, we confirmed that when the Cu-sol concentration was increased from 0.2 to 0.4 mol %, the interplanar spacing of the deposited CuO films was changed from 0.237 to 0.259 Å, and the diffraction plane of the main peak was changed from (111) to (−111). We attribute this to the fact that the interplanar spacing of Cu-sol widens with increasing CuO crystal size when the initial Cu-sol concentration is increased.

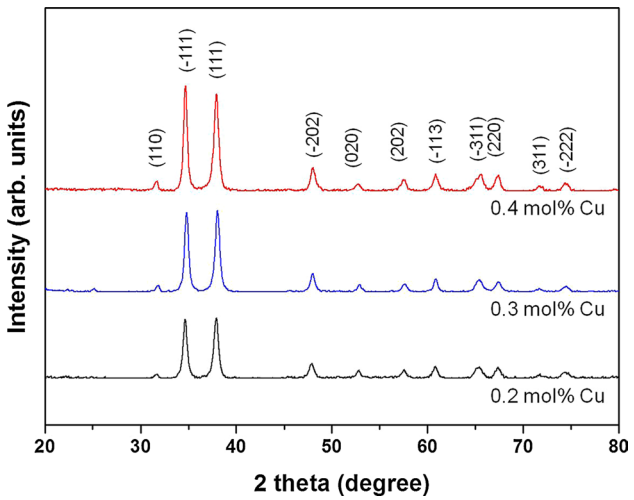

Fig. 2 XRD spectra of the CuO thin films prepared at various Cu-sol concentrations

Micrographs of the surface morphologies (Fig. 3a–d) and thicknesses (see Fig. 3, insets) of the parent glass substrates and CuO thin films were obtained. The uneven surface morphologies were confirmed by the increase in Cu concentration from 0.2 to 0.4 mol % (Fig. 3b–d) due to agglomeration and crystal growth of Cu particles during the drying and heating processes. The thickness of the 0.2 mol % CuO thin film (Fig. 3b), which was heated to 200 °C for 10 min, was approximately 55 nm when formed at a spin speed of 3000 rpm for 30 s. We observed that increasing the Cu concentration from 0.3 to 0.4 mol % resulted in an increase in CuO thin film thickness from 64 (Fig. 3c) to 76 nm (Fig. 3d). Notably, the thin film showed higher antimicrobial activity with increasing Cu concentrations on the substrate surface. EDS analysis was used to confirm the surface concentration of Cu ions. The Cu concentration in the CuO thin films ranged from 25.68–28.64 wt % (0.2–0.4 mol %) in Table 2. Figure 3e–h shows the AFM images of the parent glass and CuO thin films at various Cu concentrations. Increasing the Cu ion concentration to 0.2, 0.3, and 0.4 mol % increased the R_a of the CuO thin film to 0.227, 0.298, and 0.306 nm, respectively. Furthermore, R_t undulations increased from 18.81 to 37.80 nm (Table 2). Figure 4 shows the CAs of the parent glass and CuO thin film surfaces at various Cu concentrations. CA measurements are also a useful method for confirming R_a values [5, 9]. The parent glass had a CA value of 47.3°, as shown in Fig. 4a. On the contrary, CA values

Table 1 Crystalline size of the CuO thin film (200 °C, 10 min) generated using various Cu concentrations

Specimen	Crystalline size (nm)	FWHM (°)	D spacing (Å)	2θ (°)	Diffraction plane (hkl)
0.2 mol % Cu	5.6	1.50	0.237	37.9	(111)
0.3 mol % Cu	6.4	1.32	0.238	37.8	(111)
0.4 mol % Cu	7.6	1.09	0.259	34.7	(−111)

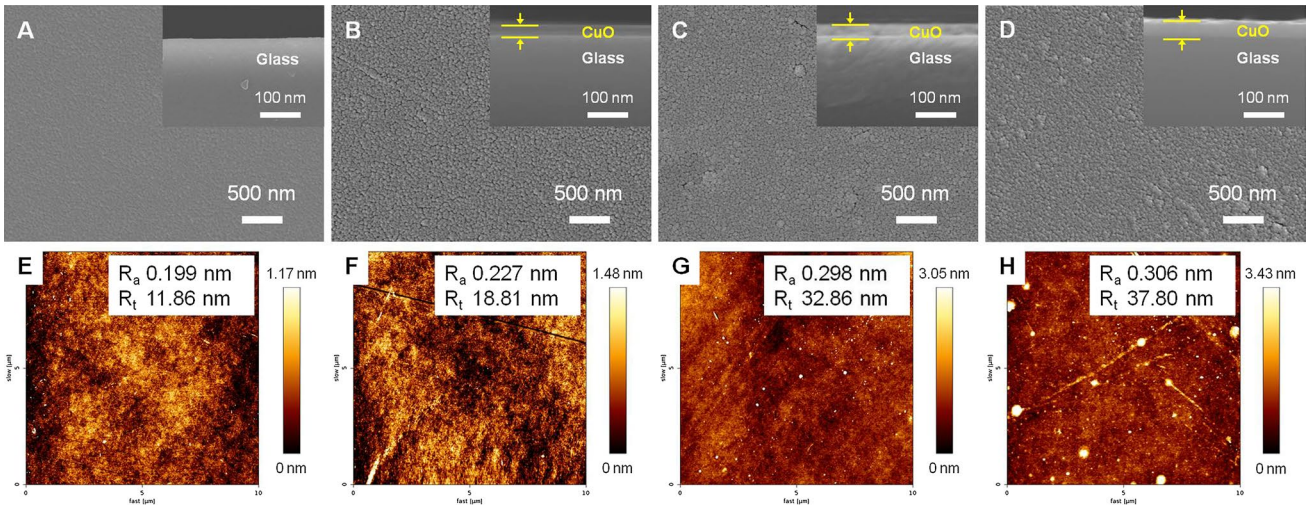

Fig. 3 Top view field emission scanning electron micrographs (**a**–**d**) and atomic force microscopy images (**e**–**h**) of CuO thin films prepared using various Cu concentrations: **a** and **e**, parent glass; **b** and **f**, 0.2 mol % Cu; **c** and **g**, 0.3 mol % Cu; **d** and **h**, 0.4 mol % Cu. The *insets* (cross-sectional views) show the thickness of the CuO thin films on the glass substrates

Table 2 EDS compositional analysis and surface roughness of the CuO thin film with various concentrations of copper sol

R_a average surface roughness, R_q root mean square roughness, R_t peak-to-valley difference

Specimen	Chemical composition (wt %)						Roughness (nm)		
	O	Si	Na	Al	Mg	Cu	R_a	R_q	R_t
Parent glass	52.68	25.91	10.70	6.25	4.46	n/a	0.199	0.265	11.86
0.2 mol % Cu	57.27	17.05	n/a	n/a	n/a	25.68	0.227	0.340	18.81
0.3 mol % Cu	56.48	15.97	n/a	n/a	n/a	27.55	0.298	0.693	32.86
0.4 mol % Cu	57.12	14.24	n/a	n/a	n/a	28.64	0.306	0.779	37.80

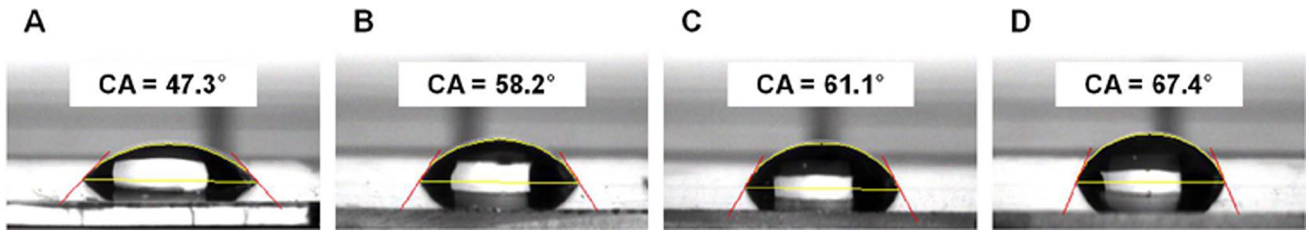

Fig. 4 Water contact angle of a drop placed on parent glass and glass coated with CuO thin films with various Cu concentrations: **a** parent glass, **b** 0.2 mol % Cu, **c** 0.3 mol % Cu, **d** 0.4 mol % Cu

of 58.2°, 61.1°, and 67.4° were obtained for the CuO thin films with Cu concentrations of 0.2, 0.3, and 0.4 mol %, respectively. The water droplet height from top to base also increased from 0.618 mm (parent glass) to 0.803 mm (0.4 mol % CuO thin film), as shown in Table 3. The results showed that as the Cu concentration increased from 0.2 to 0.4 mol %, thicker and rougher CuO films formed on the glass substrates and CA values increased. The antimicrobial activity of thin films was tested at various Cu ion concentrations because the increase in surface Cu ion concentration increased surface roughness, thereby increasing the contact surface between Cu ions and microbes.

Antibacterial and antifungal activities of CuO thin films with varying Cu ion concentrations

The numbers of colonies from four microbial strains are shown in Fig. 5 and are expressed as the logarithm of the number of colonies on the plates as a function of Cu ion concentration on the parent glass. When *E. coli* (5.565 ± 0.060 log CFU mL^{-1}), *S. aureus* (5.502 ± 0.053 log CFU mL^{-1}), *C. jejuni* (5.527 ± 0.065 log CFU mL^{-1}), and *P. funiculosum* (5.490 ± 0.040 log CFU mL^{-1}) colonies were applied to the plate, 0.2, 0.3, and 0.4 mol % CuO thin films completely inhibited bacterial growth (<1.0 log CFU mL^{-1}).

Table 3 Characteristics of CuO thin films with various Cu concentrations

Specimen	Contact angle (°)	Height (mm)	Base line length (mm)	Base area (mm^2)	Wetting energy ($mN\ m^{-1}$)
Parent glass	47.3	0.618	2.823	6.257	49.4
0.2 mol % Cu	58.2	0.721	2.596	5.293	38.3
0.3 mol % Cu	61.1	0.742	2.514	4.962	35.2
0.4 mol % Cu	67.4	0.803	2.456	4.562	28.0

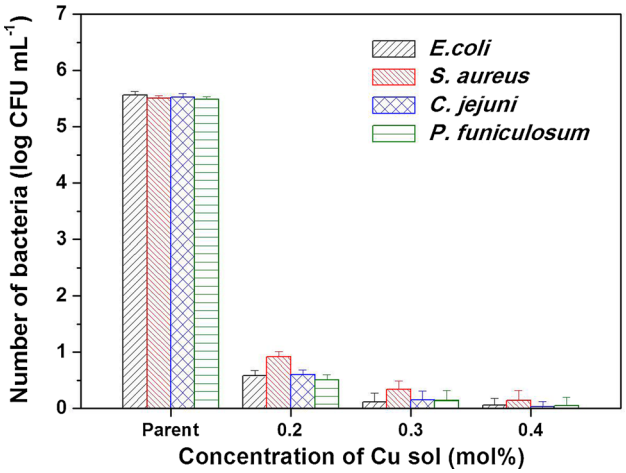

Fig. 5 Number of bacterial colonies expressed as the logarithm of the number of colonies grown on plates in the presence of parent glass or glass coated with various concentrations of Cu

Few colonies were observed at various Cu concentrations, and the minimum concentration that achieved 99.9 % antibacterial activity was 0.2 mol %. The resulting numbers of colonies for 0.2 mol % CuO film were as follows: *E. coli* (0.581 ± 0.098 log CFU mL^{-1}), *S. aureus* (0.922 ± 0.091 log CFU mL^{-1}), *C. jejuni* (0.606 ± 0.081 log CFU mL^{-1}), and *P. funiculosum* (0.509 ± 0.096 log CFU mL^{-1}). The colony numbers for 0.4 mol % CuO thin film were as follows: *E. coli* (0.060 ± 0.127 log CFU mL^{-1}), *S. aureus* (0.138 ± 0.185 log CFU mL^{-1}), *C. jejuni* (0.030 ± 0.095 log CFU mL^{-1}), and *P. funiculosum* (0.048 ± 0.151 log CFU mL^{-1}). Therefore, the antimicrobial property of the CuO thin film increased greatly with increased Cu ion concentration. As the initial Cu-sol concentration increased, the surface roughness of CuO thin films also increased, thereby increasing the contact area between the Cu ions in the CuO film and bacteria cells. As a result, the bacteria cells were destroyed by eluted Cu and active oxygen ions [18, 19]; therefore, we confirmed that the antimicrobial activities were improved.

FE-SEM analysis of bacteria and fungi treated with CuO thin film

The morphological variations in CuO film-treated bacteria and fungi were examined using FE-SEM. Figure 6a–d shows the FE-SEM images of *E. coli*, *S. aureus*, *C. jejuni*, and *P. funiculosum* cells, respectively, that were exposed to the parent glass, while Fig. 6e–h show the images of these microorganisms after exposure to 0.2 mol % CuO thin film. All microbes exposed to Cu ions were damaged in comparison to untreated microbes. In the case of *P. funiculosum* (Fig. 6d, h), the fiber aggregate shape of the fungi was untangled after Cu ion exposure. Based on these findings, it can be concluded that CuO thin films with concentrations greater than 0.2 mol % exhibited significant antimicrobial activity (99.9 %) towards *E. coli*, *S. aureus*, *C. jejuni*, and *P. funiculosum*.

Evaluation of Cu ion cytotoxicity and elution

Cytotoxicity was evaluated to test the safety of Cu ions by using NZW rabbits as an experimental model. NZW rabbits tend to show sensitivity toward test materials. The cytotoxicity of CuO thin films was determined based on PII results (Table 4). For CuO film-coated materials to be considered safe, the PII must be in the nonirritant range. In this study, the PII was calculated to be 0.0, which is within this range. After 24 and 72 h of CuO thin film exposure (Fig. 1a, b), mortality, weight fluctuations, and other effects were evaluated. After the test areas were exposed, no skin irritation such as red spots or edema was observed in the intact and abraded sites. No animals showed abnormal symptoms such as skin tinning, inflammation and skin rash during this study. Based on these results, the CuO thin films were determined to be noncytotoxic.

Evaluation of CuO film elution behavior is also an important test of the safety and durability of Cu ions. The applicability of a product can be determined based on the results of this experiment by comparing its elution behavior to the acceptable Cu ion limit (0.02–0.1 $\mu g\ L^{-1}$) in drinking water stipulated by WHO guidelines. As shown in Table 5, the Cu ion concentration was 0.014 $\mu g\ L^{-1}$ at 100 °C for 24 h in the elution test for 0.2 mol % CuO thin film, confirming that the CuO thin film satisfied the standard limit of 0.02 $\mu g\ L^{-1}$. In the case of 0.4 mol % CuO film, the maximum Cu ion concentration detected was 0.036 $\mu g\ L^{-1}$, satisfying the elution permissible range for ICP analysis. The characteristics of the 0.4 mol % CuO thin film after the elution test (100 °C for 24 h) are summarized in Table 6.

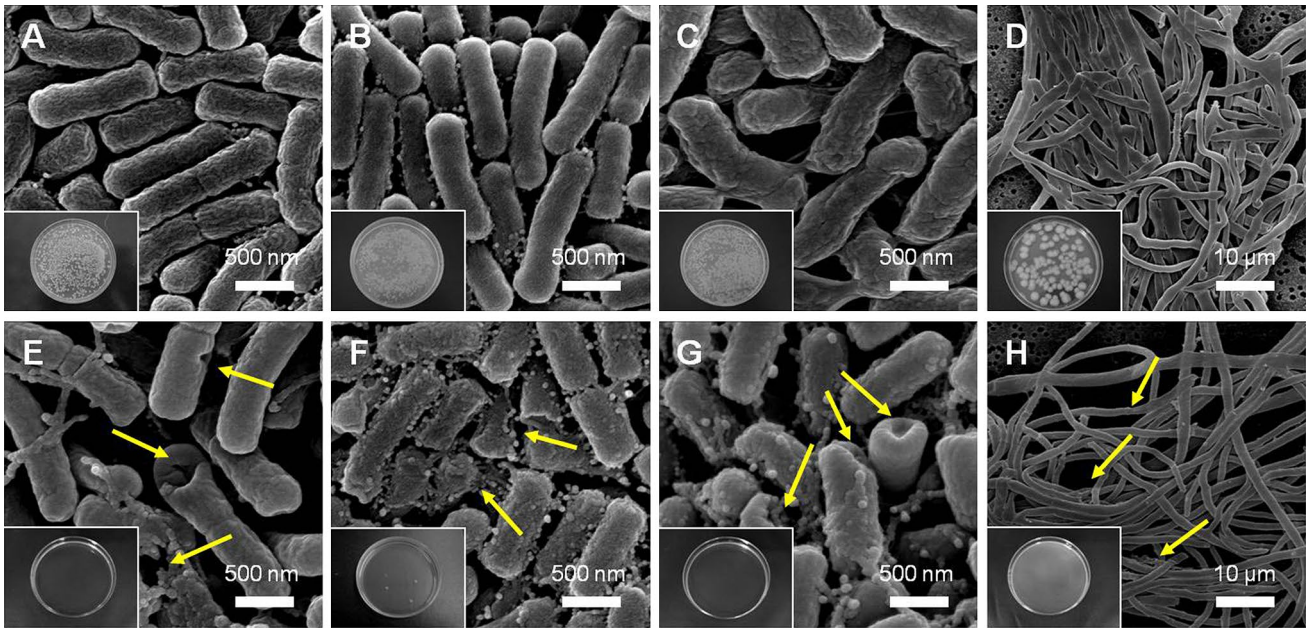

Fig. 6 FE-SEM micrographs of untreated bacteria (**a**–**d**), and those treated with 0.2 mol % CuO film (**e**–**h**) heated to 200 °C for 10 min: **a** and **e** *Escherichia coli*; **b** and **f** *Staphylococcus aureus*; **c** and **g** *Campylobacter jejuni* cells; **d** and **h** *Penicillium funiculosum* cell. The *lower left* shows photographs of bacterial colonies, which were quantified as the number of colonies present on each plate

Table 4 Cytotoxicity test results for 0.2 mol % CuO thin film

Change	Erythema and eschar				Edema			
Phases[a]	Intact		Abraded		Intact		Abraded	
	24 h	72 h	24 h	72 h	24 h	72 h	24 h	72 h
Animal number								
1	0	0	0	0	0	0	0	0
2	0	0	0	0	0	0	0	0
3	0	0	0	0	0	0	0	0
4	0	0	0	0	0	0	0	0
5	0	0	0	0	0	0	0	0
6	0	0	0	0	0	0	0	0
Sum	0	0	0	0	0	0	0	0
Mean	0.0	0.0	0.0	0.0	0.0	0.0	0.0	0.0
Sum of means	0.0							
P. I. I	0.0							

[a] Time after topical application

The residual Cu quantity on the surface decreased by more than 6.9 % from 28.64 to 26.64 wt % compared with that in the specimens before the test (Table 2). The R_a values also decreased approximately 1.6 % after the elution test due to the dissolution of Cu ions on the surface. Therefore, the CA decreased in proportion to the roughness values. The Cu composition and R_a and CA values were confirmed to decrease in the same specimens after the elution test, and the surface morphology of 0.4 mol % CuO thin film after the elution test was slightly smoothed (Fig. 7) because of the decrease in R_a. The thickness of the 0.4 mol % CuO thin film after the elution test (approximately 76 nm) was similar to that of film specimens before the test (Fig. 7a, inset).

Optical and mechanical properties of CuO thin film

Figure 8 shows the transmittance of light through CuO at various concentrations (0.2, 0.3, and 0.4 mol %) deposited on glass substrates. In order for CuO thin film to be used in display devices, high visible light transmittance of CuO-deposited glass is required. The light transmittance

Table 5 Concentration of eluted Cu ions from CuO thin films deposited on glass at 100 °C determined at various elution times (1–24 h) with inductively coupled plasma

Specimen	Concentration of eluted Cu ions ($\mu g\ L^{-1}$)				100 % eluted Cu ions ($\mu g\ L^{-1}$)[a]
	1 h	6 h	12 h	24 h	
0.2 mol % Cu	0.010	0.011	0.012	0.014	0.150
0.3 mol % Cu	0.013	0.014	0.017	0.019	0.262
0.4 mol % Cu	0.021	0.025	0.029	0.036	0.415

[a] The 100 % dissolved Cu concentration in the water with various CuO thin films (0.2–0.4 mol %) was calculated. The amount of Cu in solution for the deposited CuO films on the glass substrate was calculated using the thickness of CuO film and glass area ($10 \times 10\ mm^2$)

through the parent glass was 91.0 % at 550 nm. The transmittance of CuO thin film deposited on the glass substrate at 0.2, 0.3, and 0.4 mol % was 90.9, 90.3, and 89.6 %, respectively. Based on the Beer–Lambert law, the absorbance was found to be directly proportional to the concentration and thickness of the CuO thin film. Furthermore, the surface roughness increased with increasing concentration, thereby increasing reflectance by the scattering of surface. Therefore, the light transmittance decreased with increasing Cu ion concentration of thin film on the glass substrate. However, the light transmittance through 0.2 mol % Cu sol-coated glass that was heated to 200 °C for 10 min was similar to that of the parent glass because the oxide forms have comparatively low refractive indexes, and the thickness and surface roughness was appropriately controlled.

Discussion

Cu ions have well-known antibacterial activity, but their cytotoxicity has been examined in only a few studies. Therefore, in this study, we sought to confirm the antibacterial and antifungal properties of CuO thin films as a function of their concentration and roughness and evaluate their cytotoxicity and elution behavior. In addition, the light transmittance was measured to confirm whether CuO thin films could be applied to display devices.

In a preliminary experiment [13], the thickness of the 0.2 mol % CuO thin film increased from 31 to 91 nm when the spinning speed was decreased from 5000 to 1000 rpm. An inverse relationship between film thickness and transmittance is often observed; however, the durability of the film's antibacterial activity is relative to its thickness. Therefore, a spin speed of 3000 rpm was selected, because those two factors (durability and transmittance) should both be considered. Therefore, the CuO thin film produced from Cu-sol concentrations of 0.2, 0.3, and 0.4 mol % was then produced with thicknesses of 55, 64, and 76 nm, respectively. XRD analysis showed the CuO thin film had a monoclinic structure, without an impurity peak. When the concentration of Cu-sol was increased from 0.2 to 0.4 mol %, the interplanar spacing of the deposited CuO film increased, from 0.237 to 0.259 Å, and the diffraction plane of the main peak was changed from (111) to (−111). We attribute this to the fact that the interplanar spacing of the CuO film widened with increasing CuO crystalline size when the initial Cu-sol concentration was increased. As a result, the thickness of the CuO thin film increased proportionally with the Cu-sol concentration.

Table 6 Characteristics of CuO thin films after an elution test at 100 °C for 24 h

Specimen	Chemical composition (wt %)			Roughness (nm)			Contact angle (°)
	O	Si	Cu	R_a	R_q	R_t	
0.4 mol % Cu	58.95	14.41	26.64	0.301	0.760	34.29	62.1

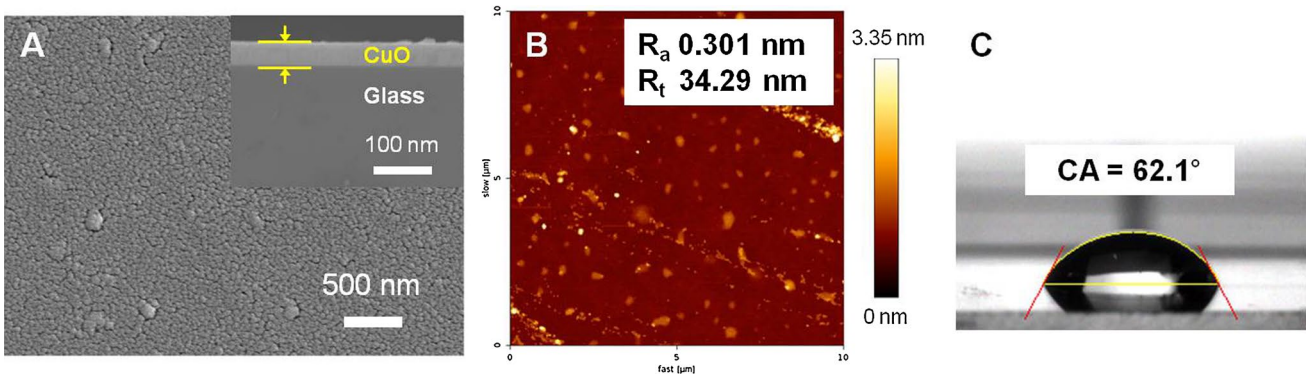

Fig. 7 Characteristics of the 0.4 mol % CuO thin film after an elution test at 100 °C for 24 h: **a** surface morphology (*inset* shows the thickness of the CuO film), **b** atomic force microscopy image, **c** water contact angle

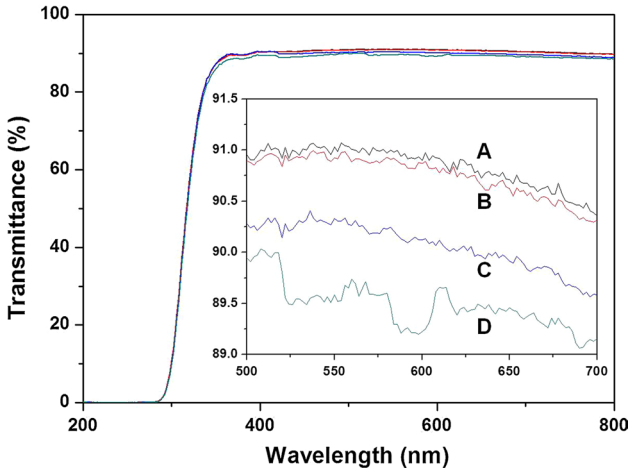

Fig. 8 Transmittance of light through the parent glass and glass coated with various CuO thin film concentrations: **a** parent glass; **b** 0.2 mol % Cu; **c** 0.3 mol % Cu; **d** 0.4 mol % Cu coated glass

When the Cu concentration increased (Fig. 3e−h), the R_a value increased slightly from 0.199 nm (parent glass) to 0.306 nm (0.4 mol % CuO thin film). Although this difference in roughness value appears slight, many reports have highlighted the influence of subnano scale roughness (smooth surface) on antibacterial activity [25, 28]. On the contrary, the R_t value increased substantially from 11.86 (parent glass) to 37.80 nm (0.4 mol % CuO thin film), which was approximately 2.2 times higher, although the thickness of CuO film was thin. To confirm the effect of roughness further, we measured the CA values of the CuO films, which increased from 47.3° (parent glass) to 67.4° (0.4 mol % CuO thin film) with increasing Cu concentration. Giljean et al. [9] have described the relationship between R_a and CA and confirmed that CA increases when the surface becomes rough due to low surface energy. The antimicrobial effects of Cu ions were related to their combination with active oxygen. The combination of Cu^+ and OH^- (active oxygen) ions destroys the membranes and DNA of microbes by interacting with proteins containing –CH and –SH groups. Therefore, the antibacterial and antifungal activities increased when the concentration of Cu-sol was increased from 0.2 to 0.4 mol %, because the increase in Cu-sol concentration increased the roughness of the CuO film, increasing the contact surface between Cu ions and microbes. Interestingly, at 0.2 mol % Cu, the number *S. aureus* colonies (0.922 ± 0.091 log CFU mL^{-1}) was slightly higher than that of *E. coli* (0.581 ± 0.098 log CFU mL^{-1}) and *C. jejuni* (0.606 ± 0.081 log CFU mL^{-1}). Therefore, CuO thin film had greater antibacterial activity towards Gram-negative bacteria such as *E. coli* and *C. jejuni* than on Gram-positive bacteria such as *S. aureus*. This is because Gram-positive bacteria have cell walls with a relatively thicker peptidoglycan layer. These observations are in accordance with the positive effect theory reported by Akira et al. [24].

The toxicity of Cu ions was determined by performing experiments on an animal model. The Cu ions were found to be noncytotoxic. When the nanoscale Cu ions are eluted from the CuO thin film, bacterial cell walls can be destroyed by the cation effect. However, during the cytotoxicity test, CuO thin film was found to be non-cytotoxic to the epidermis and dermis within the 24–72 h treatment period. Although the test site was large (2.5×2.5 cm^2), the minimum concentration of eluted Cu ions (0.014–0.036 μg L^{-1}) at the antimicrobial concentration (0.2–0.4 mol %) was controlled by heating to 200 °C for 10 min. The concentration of eluted Cu ions is related to the diffusion process, and is directly proportional to concentration, temperature, humidity, and maintenance time. The quantity of eluted ions increased proportionately with increasing Cu-sol concentration and heating time. Cu ions were eluted at 0.036 μg L^{-1} from 0.4 mol % CuO thin film, which was within the acceptable elution range for ICP analysis. In addition, the calculated 100 % dissolved Cu concentration in water with various CuO thin films (0.2, 0.3, and 0.4 mol % Cu) was approximately 0.150, 0.262, and 0.415 μg L^{-1}, respectively (Table 5). The dissolved Cu concentrations during the elution test (100 °C for 24 h) with various CuO thin films (0.2–0.4 mol % Cu) were 9.3, 7.2, and 8.7 % of the total (100 % dissolved Cu concentration), respectively. Therefore, we confirmed the chemical stability of CuO thin films under extreme conditions (100 °C, 24 h) during the elution test. Based on the results of the cytotoxicity and elution tests, we conclude that the CuO thin films manufactured at various concentrations were non-irritating, chemical stability, and satisfied the WHO elution guidelines (2.0 mg L^{-1}) for drinking water.

Conclusions

To summarize, CuO thin films with different concentrations and roughness values were generated using a sol–gel method, and the antimicrobial (bacteria and fungi) activities, cytotoxicity, and elution behavior were examined using *E. coli*, *S. aureus*, *C. jejuni* and *P. funiculosum*. The CuO thin films showed excellent antimicrobial activities (99.9 %) at Cu concentrations greater than 0.2 mol % Cu, and that the antimicrobial activity of the CuO thin films was related to their concentrations and roughness values, which affected the contact surface between the Cu ions and microbes. The cytotoxicity tests demonstrated that the CuO thin film was noncytotoxic. The quantity of eluted Cu ions was 0.014 μg L^{-1} from 0.2 mol % CuO thin film, which satisfies the drinking water elution guidelines of the WHO. The transmittance of light through 0.2 mol % CuO film-deposited glass was 90.9 %. The antimicrobial activity, cytotoxicity, elution, and transmittance of CuO-deposited

glass suggest that Cu ions have valuable applications in various fields, including in the manufacturing of mobile phones, touch panels, and electrical appliances.

Acknowledgments The authors would like to thank Prof. Kwang-Mahn Kim and Dr. Yu-Ri Choi from the Yonsei University College of Dentistry for their technical assistance.

Conflict of interest The authors declare that they have no conflict of interest.

References

1. Boveris A, Musacco-Sebio R, Ferrarotti N, Saporito-Magriñá C, Torti H, Massot F, Repetto MG (2012) The acute toxicity of iron and copper: biomolecule oxidation and oxidative damage in rat liver. J Inorg Biochem 116:63–69
2. Brown NL, Rouch DA, Lee BTO (1992) Copper resistance determinants in bacteria. Plasmid 27:41–51
3. Byarugaba DK (2004) A view on antimicrobial resistance in developing countries and responsible risk factors. Int J Antimicrob Agents 24:105–110
4. Cao XL, Cheng C, Ma YL, Zhao CS (2010) Preparation of silver nanoparticles with antimicrobial activities and the researches of their biocompatibilities. J Mater Sci Mater Med 21:2861–2868
5. Chen H, Wang W, Li G, Li C, Zhang Y (2011) Synthesis of P(St-MAA)-Fe_3O_4/Ppy core − shell composite microspheres with conductivity and superparamagnetic behaviors. Synth Met 161:1921–1927
6. Djemai-Zoghlache Y, Isambert A, Belhaneche-Bensemra N (2011) Electrochemical behavior of the 316L steel type in a marine culture of microalgae (Porphyridium purpureum) under the 12/12 h photoperiod and effect of different working electrode exposure conditions on the biofilm–metal interface. J Ind Microbiol Biotechnol 38:1969–1978
7. Djeribi R, Bouchloukh W, Jouenne T, Menaa B (2012) Characterization of bacterial biofilms formed on urinary catheters. Am J Infect Control 40:854–859
8. Drake PL, Hazelwood KJ (2005) Exposure-related health effects of silver and silver compounds: a review. Ann Occup Hyg 49:575–585
9. Giljean S, Bigerelle M, Anselme K, Haidara H (2011) New insights on contact angle/roughness dependence on high surface energy materials. Appl Surf Sci 257:9631–9638
10. He L, Liu Y, Mustapha A, Lin M (2011) Antifungal activity of zinc oxide nanoparticles against *Botrytis cinerea* and *Penicillium expansum*. Microbiol Res 166:207–215
11. Jiang Q, Jiang Z, Ma K, Li R, Du J, Xie Z, Huang TS (2014) Development of cytocompatible antibacterial electro-spun nanofibrous composites. J Mater Sci 49:6734–6741
12. Kaliaraj GS, Ramadoss A, Sundaram M, Balasubramanian S, Muthirulandi J (2014) Studies of calcium-precipitating oral bacterial adhesion on TiN, TiO_2 single layer, and TiN/TiO_2 multilayer-coated 316L SS. J Mater Sci 49:7172–7180
13. Kim YH, Choi YR, Kim KM, Choi SY (2012) Evaluation of copper ion of antibacterial effect on *Pseudomonas aeruginosa*, *Salmonella typhimurium* and *Helicobacter pylori* and optical, mechanical properties. Appl Surf Sci 258:3823–3828
14. Kumar R, Münstedt H (2005) Silver ion release from antimicrobial polyamide/silver composites. Biomaterials 26:2081–2088
15. Kumar R, Sidhu MK, Ganguly NK, Chakraborti A (1999) Identification of Copper-Zinc superoxide dismutase gene from enteroaggregative *Escherichia coli*. Microbiol Immunol 43:481–484
16. Lakouraj MM, Rahpaima G, Mohseni SM (2013) Synthesis, characterization, and biological activities of organosoluble and thermally stable xanthone-based polyamides. J Mater Sci 48:2520–2529
17. Mahltig B, Fiedler D, Böttcher H (2004) Antimicrobial sol–gel coatings. J Sol-Gel Sci Technol 32:219–222
18. Ochi K, Tanaka Y, Tojo S (2014) Activating the expression of bacterial cryptic genes by rpoB mutations in RNA polymerase or by rare earth elements. J Ind Microbiol Biotechnol 41:403–414
19. Okeke IN, Klugman KP, Bhutta ZA, Duse AG, Jenkins P, O'Brien F, Pablos-Mendez A, Laxminarayan R (2005) Antimicrobial resistance in developing countries. Part II: strategies for containment. Lancet Infect Dis 5:568–580
20. Olivares M, Pizarro F, Speisky H, Lönnerdal B, Uauy R (1998) Copper in infant nutrition: safety of World Health Organization provisional guideline value for copper content of drinking water. J Pediatr Gastroenterol Nutr 26:251–257
21. Parikh DV, Fink T, Rajasekharan K, Sachinvala ND, Sawhney APS, Calamari TA (2005) Antimicrobial silver/sodium carboxymethyl cotton dressings for burn wounds. Text Res J 75:134–138
22. Ren G, Hu D, Cheng EW, Vargas-Reus MA, Reip P, Allaker RP (2009) Characterisation of copper oxide nanoparticles for antimicrobial applications. Int J Antimicrob Agents 33:587–590
23. Stanić V, Janaćković D, Dimitrijević S, Tanasković SB, Mitrić M, Pavlović MS, Krstić A, Jovanović D, Raićević S (2011) Synthesis of antimicrobial monophase silver-doped hydroxyapatite nanopowders for bone tissue engineering. Appl Surf Sci 257:4510–4518
24. Takeuchi O, Hoshino K, Kawai T, Sanjo H, Takada H, Ogawa T, Takada H, Akira S (1999) Differential roles of TLR2 and TLR4 in recognition of gram-negative and gram-positive bacterial cell wall components. Immunity 11:443–451
25. Truong VK, Lapovok R, Estrin YS, Rundell S, Wang JY, Fluke CJ, Crawford RJ, Ivanova EP (2010) The influence of nano-scale surface roughness on bacterial adhesion to ultrafine-grained titanium. Biomaterials 31:3674–3683
26. Vorotilov K, Petrovoksy V, Vasiljev V (1995) Spin coating process of sol-gel silicate films deposition: effect of spin speed and processing temperature. J Sol-Gel Sci Technol 5:173–183
27. Wang F, Guo C, Liu CZ (2013) Immobilization of Trametes versicolor cultures for improving laccase production in bubble column reactor intensified by sonication. J Ind Microbiol Biotechnol 40:141–150
28. Yang C, Tartaglino U, Persson BNJ (2006) Influence of surface roughness on superhydrophobicity. Phys Rev Lett 97:116103
29. Yukitake H, Naito M, Sato K, Shoji M, Ohara N, Yoshimura M, Sakai E, Nakayama K (2011) Effects of non-iron metalloporphyrins on growth and gene expression of Porphyromonas gingivalis. Microbiol Immunol 55:141–153
30. Zhang B, Lin Y, Tang X, Suqiong HE, Xie X (2010) Synthesis, characterization, and antimicrobial properties of Cu-inorganic antibacterial material containing lanthanum. J Rare Earths 28:451–455
31. Zhang C, Li C, Chen Y, Zhang Y (2014) Synthesis and catalysis of Ag nanoparticles trapped into temperature-sensitive and conductive polymers. J Mater Sci 49:6872–6882